

Structural correlations tailor conductive properties in polymerized ionic liquids

Benjamin Doughty^{1*}, Anne-Caroline Genix^{2*}, Ivan Popov¹, Bengrui Li³, Sheng Zhao³, Tomonori Saito¹, Daniel A. Lutterman¹, Robert L. Sacchi¹, Bobby G. Sumpter^{4,5}, Zaneta Wojnarowska^{1,6}, Vera Bocharova^{1*}

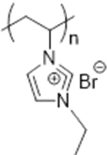
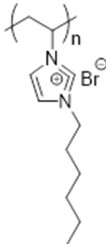

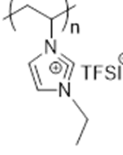
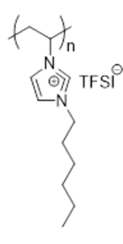
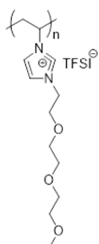
AUTHOR ADDRESS:

1. Chemical Sciences Division, Oak Ridge National Laboratory, Oak Ridge, TN 37831, USA
2. Laboratoire Charles Coulomb (L2C), Université de Montpellier, CNRS, F-34095 Montpellier, France
3. Department of Chemistry, University of Tennessee, Knoxville, Tennessee 37996, United States
4. Center for Nanophase Materials Sciences, Oak Ridge National Laboratory, Oak Ridge, Tennessee 37831, US
5. Computational Sciences & Engineering Division, Oak Ridge National Laboratory, Oak Ridge, Tennessee 37831, USA
6. Institute of Physics, University of Silesia, SMCEBI, 75 Pulku Piechoty 1A, 41-500 Chorzow, Poland

Summary of fitting of WAXS spectra

The repeating distances in real space for d_{anion} and d_{pendant} , and $\xi_{\text{anion}}/d_{\text{anion}}$ and $\xi_{\text{pendant}}/d_{\text{pendant}}$ are summarized in Table S1.

Table S1: Results of WAXS data fitting.

| | A1 | B1 | C1 | A2 | B2 | C2 |
|---|---|---|---|--|---|---|
| |  |  |  |  |  |  |
| d_{anion} , nm (WAXS) | 0.561 ± 0.001 | | | 0.693 ± 0.003 | 0.779 ± 0.002 | 0.642 ± 0.002 |
| d_{pendant} , nm (WAXS) | 0.371 ± 0.002 | 0.376 ± 0.002 | 0.378 ± 0.003 | 0.457 ± 0.003 | 0.450 ± 0.002 | 0.438 ± 0.004 |
| $\xi_{\text{anion}}/d_{\text{anion}}$ (WAXS) | 5.66 ± 0.24 | | | 2.88 ± 0.31 | 1.98 ± 0.28 | 1.98 ± 0.22 |
| $\xi_{\text{pendant}}/d_{\text{pendant}}$ (WAXS) | 1.99 ± 0.21 | 2.11 ± 0.21 | 2.65 ± 0.23 | 1.93 ± 0.26 | 2.36 ± 0.21 | 2.29 ± 0.22 |

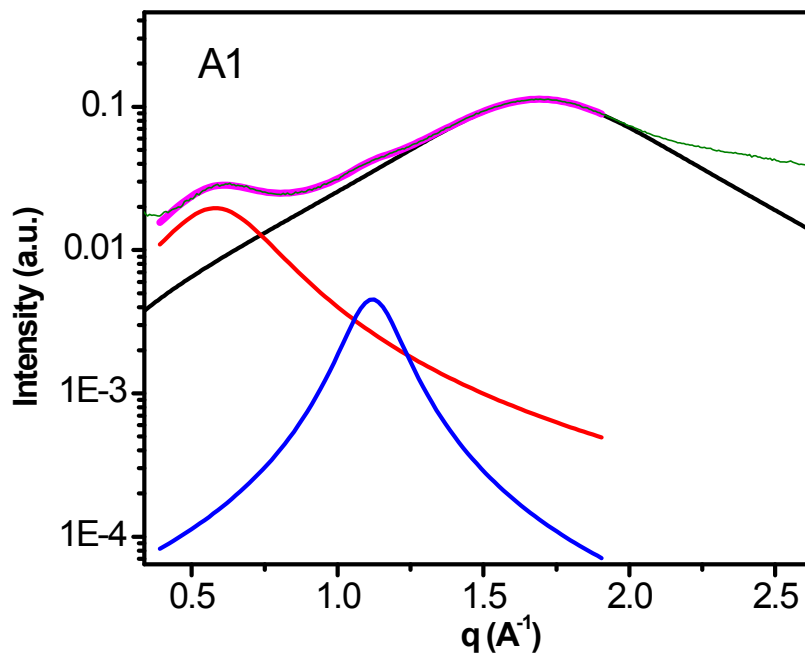


Figure S1: Example of fitting of WAXS spectra for Al.

vSFG Experimental Description:

The output of a Spectra Physics Spitfire Pro Ti:Sapphire amplifier producing ~6 W average power, running at a 1 kHz repetition rate producing ~40 fs pulses centered at 799.8 nm was split into two paths. One path was directed into a TOPAS-Prime Plus optical parametric amplifier and difference frequency mixer to produce mid-IR light centered at 2900 cm⁻¹ with roughly a 300 cm⁻¹ bandwidth at full width at half maximum. Approximately 1.2 W of the second arm was directed into a 4f-pulse shaper with a mechanical slit placed at the Fourier plane to generate ~1 ps near infrared (NIR) pulses used for up-conversion. The IR and NIR beams were overlapped in space and in time at the sample position with incident angles of 66° and 48°, respectively, with respect to the surface normal. Approximately 4 mW of NIR laser power was used in experiments, as measured at the sample position, whereas 14.6 mW of mid-IR power was used. The radiated vSFG was collimated, polarization resolved and filtered with a 750 nm short pass before being focused into the entrance of a spectrograph equipped CCD camera. Two polarization combinations were collected for each sample – SSP and PPP, where the letters in the abbreviation describes the polarization of light measured/used in experiments in decreasing energy (i.e., SSP = S-SFG, S-NIR, P-IR). For all data

presented, vSFG spectra were background subtracted using a co-specified region of interest to remove stray light and the CCD camera intensity offset. Several frames were averaged together and to establish reproducibility in the measurement and that the samples were not damaged during measurements. The background subtracted spectra were then scaled by a non-resonant response from an Au film in the PPP combination to account for the spectral shape of the driving IR pulse. Considering associated Fresnel factors and the thickness of the samples probed in this work the vSFG measurements presented here are representative of the air-PolyIL interface.

vSFG Spectral Assignment and Summary of Fitting Parameters:

Here, we elaborate on the assignments on the C-type polymers. To start, DFT calculations predict that the asymmetric stretch of the terminal methyl groups of the tails in C1 and C2 polymers should be found near 2965 cm^{-1} ; indeed, bands found near 2952 cm^{-1} are observed in the SFG spectra and are tentatively assigned to this mode. It should be noted however that DFT calculations indicate that the terminal methyl group is not ‘pure’ but rather is composed of substantial contributions from a nearby methylene group. This is apparent in the frequency in which the $\text{-CH}_3\text{-ss}$ is predicted to be found: $\sim 2798\text{ cm}^{-1}$, which is much redder than what one would expect for a pure $\text{-CH}_3\text{-ss}$ and is redder than the $\text{-CH}_2\text{-ss}$ modes of the tail. Notably, no SFG signal is observed in the 2800 cm^{-1} region and only weak features/shoulders are found in the IR/Raman spectra (supplied in the SI below) that cannot be definitively assigned to this vibration. Instead the strong band at $\sim 2875\text{ cm}^{-1}$ in the vSFG spectra is tentatively attributed to the terminal methyl symmetric stretch group on the side chain based on the strength in the SSP spectrum, a corresponding absence in the PPP spectrum, and the absence in the A2 PolyILs that do not have this side group. This leaves features near $\sim 2942\text{ cm}^{-1}$ in the SFG spectra that are mostly likely due to a Fermi resonance, based on good agreement with the work of Baldelli and coworkers.¹

For A2 and APF_6 PolyILs (data shown in Figure S1) the peaks observed near 2996 cm^{-1} are attributed to the asymmetric stretch of the methylene groups on the polymer backbone, whereas the peaks at 2963 cm^{-1} are assigned to the $\text{-CH}_3\text{-as}$ of from the ethyl side group. For these polymers, we observe far fewer peaks in the vSFG spectra with a much weaker overall intensity as compared to those C-type PolyILs discussed above. This is descriptive of an overall cancelation of vSFG

signals due to local symmetry and is descriptive of better overall packing. Lower frequency modes, such as those found near $\sim 2900\text{ cm}^{-1}$ and $\sim 2940\text{ cm}^{-1}$ are tentatively assigned to tail $-\text{CH}_2\text{-ss}$ modes and tail $-\text{CH}_3\text{-ss}$ /Fermi resonance, respectively based on their observed frequencies. Notably, changing the anion from a small symmetric PF_6^- to TFSI^- (for A2), we can see the impact of the polymer ordering as missing features between the two spectra (e.g., tail $-\text{CH}_3\text{-ss}$ /Fermi resonance peak near 2940 cm^{-1}) and lower overall signals. This indicates that the TFSI^- containing polymer is more ordered than the PF_6^- containing polymer suggesting that the reduction in anion size leads to worsening in the polymer packing. This result agrees with the X-ray measurements described above because PF_6^- anions are only slightly larger than the Br^- anions.

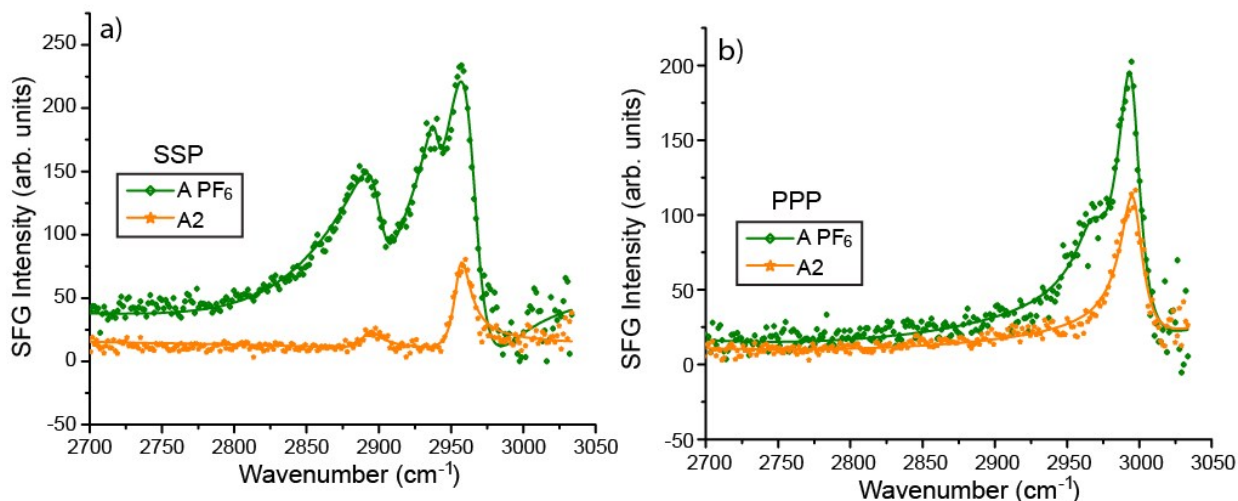


Figure S2: vSFG spectra from APF6 and A2 PolyILs.

Fitting parameters and associated assignments from vSFG spectra are summarized below along with relevant results from DFT normal mode calculations for the PolyIL trimer (where available). Error bars on parameters are obtained from the uncertainty in the fitting.

Table S2: Fitting parameters and associated assignments from vSFG combined with DFT calculations

| C1 | | | | | Theory (Scaled) |
|---------------------------------------|------------|----------------|------------------------------|------------------------------|------------------------------|
| Assignment | Pol. Comb. | A (arb.unit) | ω (cm ⁻¹) | Γ (cm ⁻¹) | ω (cm ⁻¹) |
| Tail -CH ₂ - <i>ss</i> | PPP | -101.1 ± 4.0 | 2817.9 ± 0.3 | 24.3 ± 0.8 | 2828.9 |
| Tail -CH ₂ - <i>ss</i> | SSP | 229.7 ± 1.3 | 2826.6 ± 0.1 | 11.0 ± 0.1 | 2828.9 |
| Tail -CH ₃ - <i>ss</i> | SSP | 273.5 ± 6.1 | 2874.9 ± 0.2 | 25.0 ± 0.4 | |
| Tail -CH ₂ - <i>as</i> | PPP | 185.5 ± 3.9 | 2886.1 ± 0.3 | 26.7 ± 0.4 | 2883.2 |
| backbone -CH ₂ - <i>ss</i> | SSP | 22.5 ± 1.9 | 2900.5 ± 0.2 | 6.0 ± 0.4 | 2892.1 |
| FR | SSP | 185.9 ± 30.8 | 2942.0 ± 1.9 | 22.9 ± 0.7 | - |
| Tail -CH ₃ - <i>as</i> | PPP | -31.5 ± 1.5 | 2948.5 ± 0.2 | 8.0 ± 0.4 | 2965.2 |
| Tail -CH ₃ - <i>as</i> | SSP | 160.6 ± 26.0 | 2953.4 ± 0.3 | 13.1 ± 0.7 | 2965.2 |
| Backbone CH ₂ - <i>as</i> | PPP | 95.9 ± 3.3 | 2986.1 ± 0.2 | 16.8 ± 0.4 | 2976.1 |

| C2 | | | | | Theory (Scaled) |
|-----------------------------------|------------|----------------|------------------------------|------------------------------|------------------------------|
| Assignment | Pol. Comb. | A (arb.unit) | ω (cm ⁻¹) | Γ (cm ⁻¹) | ω (cm ⁻¹) |
| Tail -CH ₂ - <i>ss</i> | SSP | 133.1 ± 1.8 | 2827.5 ± 0.1 | 13.3 ± 0.1 | 2831.4 |
| Tail -CH ₂ - <i>ss</i> | PPP | -120.0 ± 9.6 | 2835.3 ± 2.3 | 38.6 ± 2.2 | 2831.4 |
| Tail -CH ₃ - <i>ss</i> | SSP | 73.2 ± 1.9 | 2876.0 ± 0.1 | 12.5 ± 0.3 | |
| Tail -CH ₂ - <i>as</i> | PPP | 93.4 ± 5.2 | 2891.0 ± 1.3 | 22.4 ± 1.1 | 2883.7 |
| FR | SSP | 151.0 ± 10.9 | 2928.4 ± 0.6 | 36.7 ± 1.6 | |

| APF6 | | | | |
|-------------|------------|----------------|------------------------------|------------------------------|
| Assignment | Pol. Comb. | A (arb.unit) | ω (cm ⁻¹) | Γ (cm ⁻¹) |

| | | | | |
|--|-----|-------------|--------------|------------|
| Tail -CH ₂ - <i>ss</i> | SSP | 43.6 ± 2.1 | 2900.5 ± 0.1 | 11.1 ± 0.4 |
| Tail -CH ₃ - <i>ss</i> / FR | SSP | 11.4 ± 0.8 | 2940.1 ± 0.1 | 5.6 ± 0.3 |
| Tail -CH ₃ - <i>as</i> | SSP | 154.8 ± 2.0 | 2964.0 ± 0.1 | 12.8 ± 0.1 |
| Tail -CH ₃ - <i>as</i> | PPP | 23.8 ± 2.3 | 2969.8 ± 0.3 | 11.7 ± 0.8 |
| Backbone CH ₂ - <i>as</i> | PPP | 90.2 ± 1.3 | 2995.2 ± 0.1 | 9.6 ± 0.1 |

| | | | | |
|--------------------------------------|------------|---------------------|------------------------------|------------------------------|
| A2 | | | | |
| Assignment | Pol. Comb. | <i>A</i> (arb.unit) | ω (cm ⁻¹) | Γ (cm ⁻¹) |
| Tail -CH ₂ - <i>ss</i> | SSP | 25.2 ± 1.6 | 2892.5 ± 0.6 | 7.6 ± 0.6 |
| Tail -CH ₃ - <i>as</i> | SSP | 79.0 ± 1.4 | 2955.9 ± 0.1 | 6.9 ± 0.1 |
| Backbone CH ₂ - <i>as</i> | PPP | 116.8 ± 0.9 | 2996.5 ± 0.1 | 9.4 ± 0.1 |

Linear Vibrational Spectroscopy:

For comparison, conventional linear Raman and attenuated total internal reflection Fourier transform infrared (ATR-FTIR) spectra from the *same* samples probed in SFG measurement are shown in Figure S2 and S3, respectively. Notably, the number of bands clearly observed are fewer, with many weaker bands buried or convoluted with more intense features. This is expected from linear spectroscopic methods where the heterogeneous broadening from the assortment of local chemical environments probed in the bulk sample are averaged over. In contrast, the vSFG measurements probe only species near the interface thus limiting the heterogeneous broadening in the associated spectra. For the low C-type polymers, clear peaks in the Raman spectra are found near 2838 cm⁻¹, 2883 cm⁻¹ and 2952 cm⁻¹ in the vertical polarization scheme (Figure S2b), which corresponds to those bands assigned in the vSFG spectrum and summarized in the above tables. In the horizontal polarization spectra (Figure S2b) peaks at 2865 cm⁻¹ and 2942 cm⁻¹ are found. The A-type samples show Raman signals in the vertical spectra (Figure S2c) near 2893 cm⁻¹, 2951 cm⁻¹, and 2997 cm⁻¹. Raman show peaks in the horizontal polarization are found at 2953 cm⁻¹ and 2970 cm⁻¹. The ATR-FTIR spectra are broader still, even with the often-assumed surface sensitivity of the ATR geometry, the penetration depth of the evanescent wave is many microns

into the bulk and thus averages over many local environments. Bands in the IR spectra from C-type polymers can be identified at $\sim 2838\text{ cm}^{-1}$, $\sim 2884\text{ cm}^{-1}$, and $\sim 2934\text{ cm}^{-1}$ that correspond to the modes assigned using vSFG selection rules and DFT normal modes. Likewise, A-type polymers show weak bands at $\sim 2947\text{ cm}^{-1}$ and $\sim 2991\text{ cm}^{-1}$.

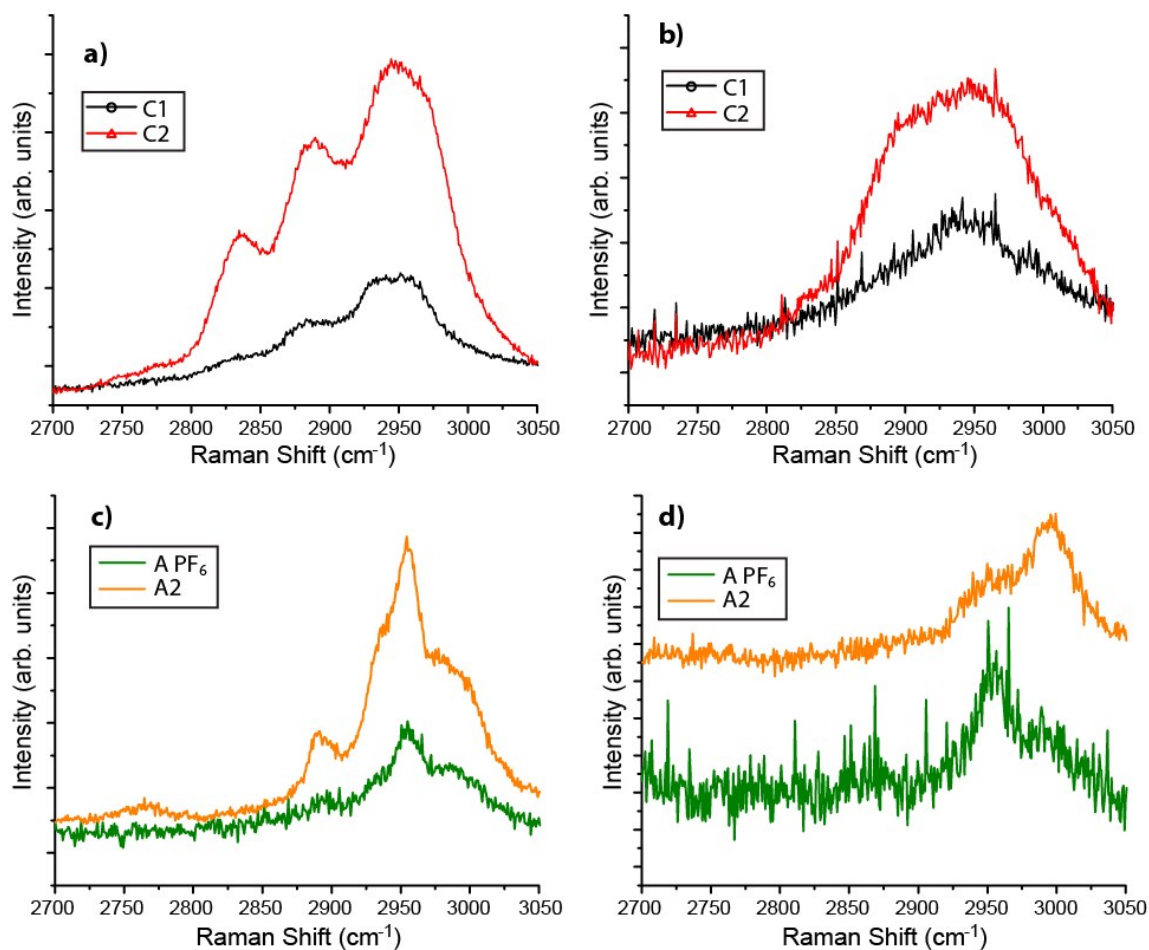


Figure S3: Polarized Raman measurements for the PolyILs samples studied in this work. a) and b) show SFG data from the B-type PolyILs, while c) and d) are spectra from the high A-type PolyIL species. The left column is vertically polarized Raman, and the right is horizontally polarized.

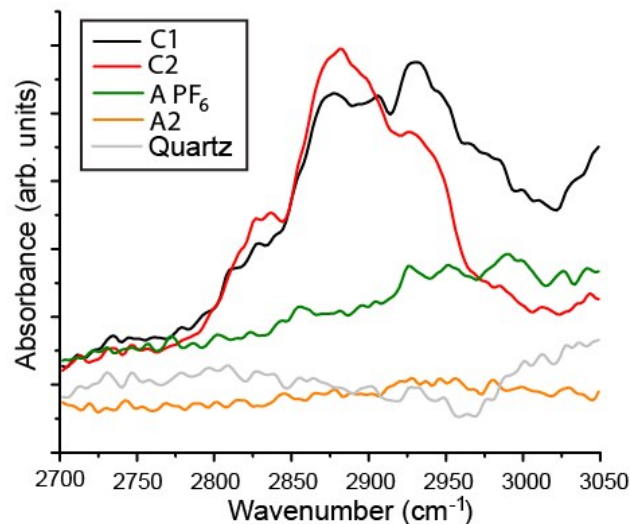


Figure S4: ATR-FTIR spectra for the PolyILs samples described in the text and SI.

Summary of BDS measurements

Fig. S4 presents the temperature dependence of the dc-conductivity for all studied PolyILs. All samples reveal similar behavior of σ_{dc} : a decrease in temperature results in changing the conductivity behavior from a VFT-like to an Arrhenius type with a characteristic crossover observed at a temperature related to T_g for the given system. To extract E_a at $T < T_g$ we fitted the data with Arrhenius equation, $\sigma = \sigma_0 \exp(-E_a/kT)$ or results in Fig S4 below T_g were fitted by $\log \sigma = \log \sigma_0 + (0.4343 \cdot E_a \cdot 1000/T)/R$, where R is the gas constant. The example of fitting with Vogel-Fulcher-Tamman (VFT) and Arrhenius is presented for A2, the slope corresponds to $E_a = 110 \text{ kJ/mol}$

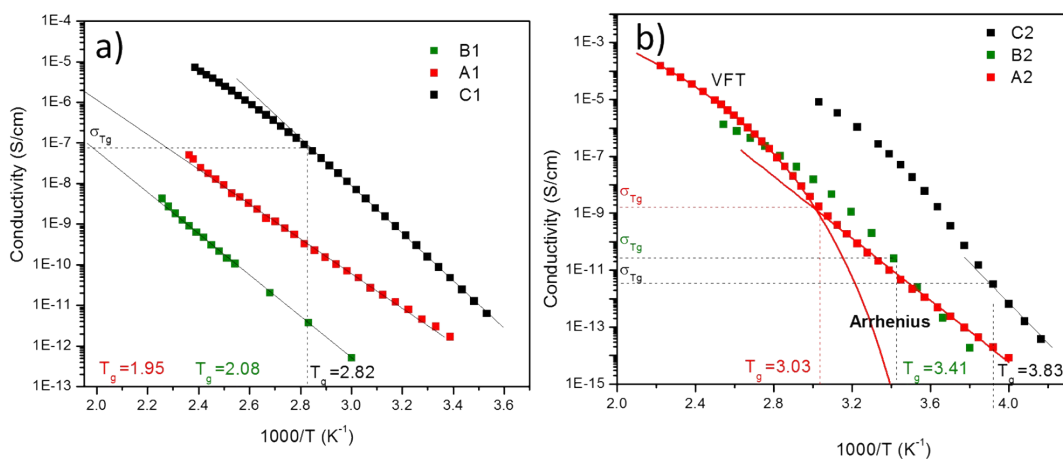


Figure S5: BDS spectra for Br a) and TFSI b) containing PolyILs. The B parameter from VFT is 1869K, 1405K, 860K, and 1800K for A2, B2, C2, and C1 respectively. Furthermore, for A1 and B1 only Arrhenius regime was detected in BDS. This is also supported by their very high values of T_g (close to the sample degradation) obtained from DSC.

DSC measurements

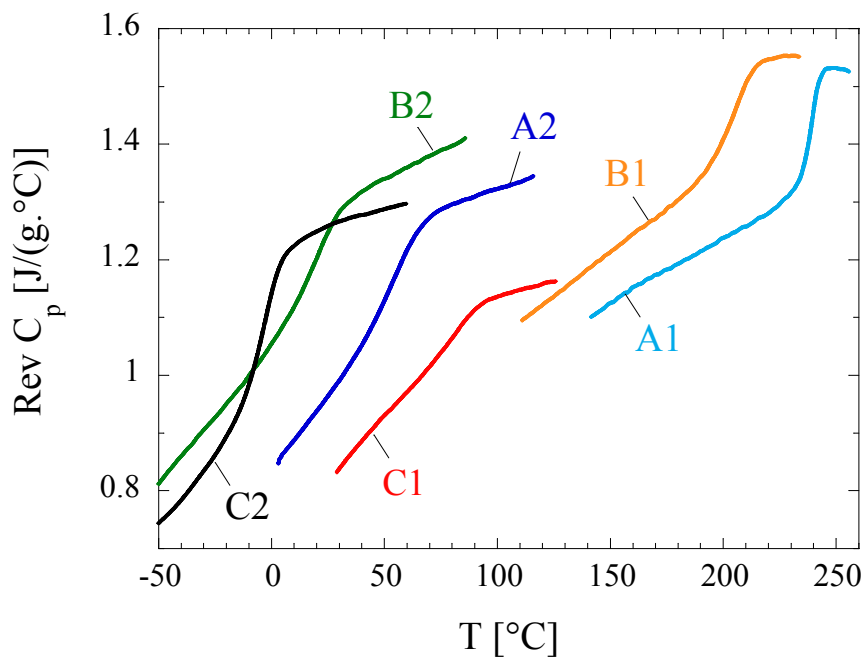


Figure S6: Heat capacity measured by DSC for PolyILs

DFT calculations

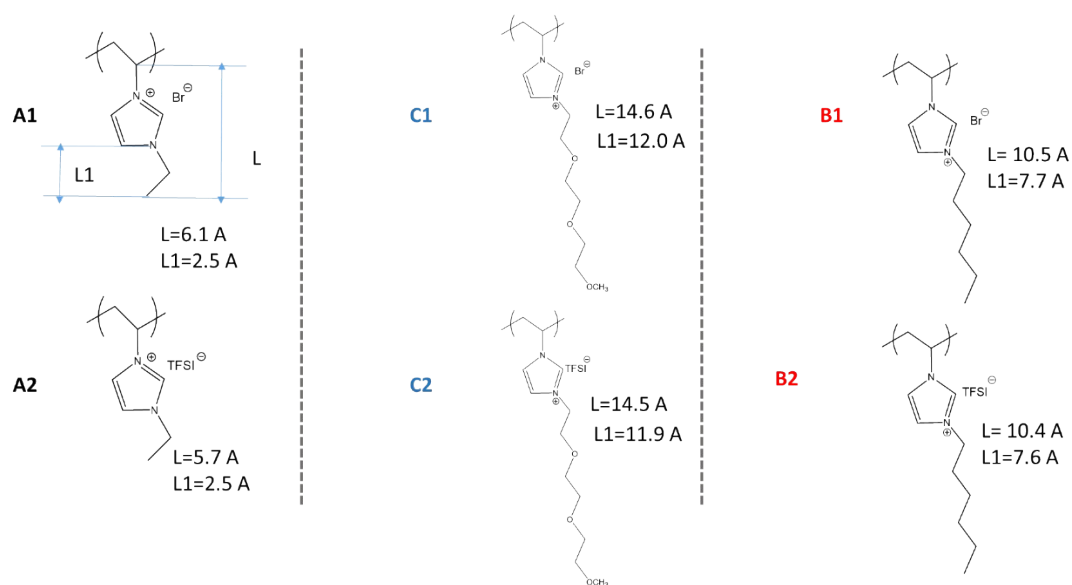


Figure S7: Characteristic length of the tail (L1) and length of pendant/side groups (L) obtained from DFT Optimized Structures

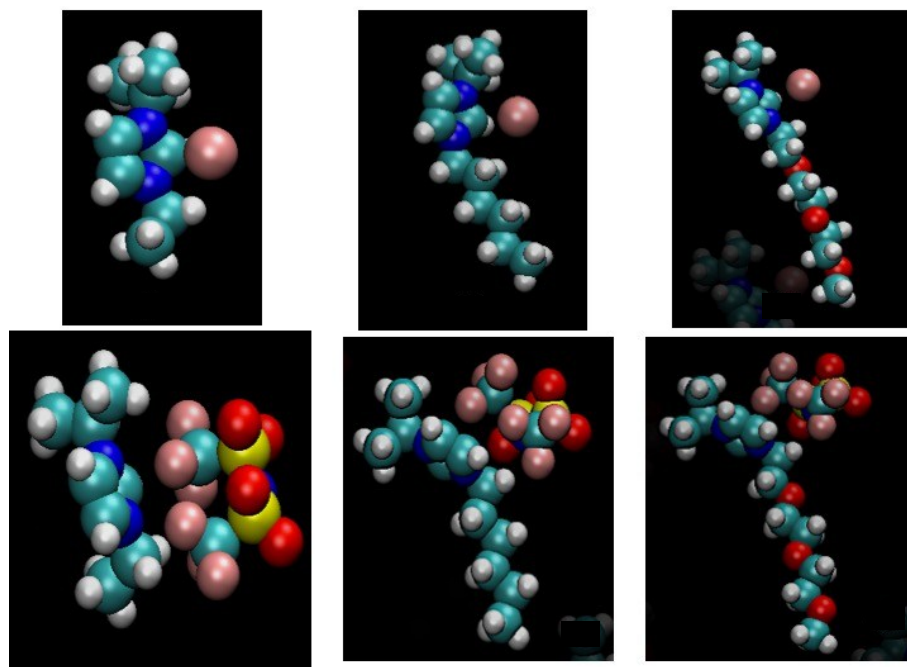


Figure S8: Full molecule structures from DFT. In the first row from right to left are structures A1, C1, B1, while structures A2, C2, B2 are on the second row.

1. Aliaga, C.; Santos, C. S.; Baldelli, S., Surface chemistry of room-temperature ionic liquids. *Phys. Chem. Chem. Phys.* **2007**, 9 (28), 3683-3700.